Biochemical and Biophysical Research Communications 412 (2011) 8–12

Contents lists available at ScienceDirect

Biochemical and Biophysical Research Communications

journal homepage: www.elsevier.com/locate/ybbrc

Transmembrane molecular transport during versus after extremely large, nanosecond electric pulses

Kyle C. Smith [a,b], James C. Weaver [a,*]

[a] Harvard-M.I.T. Division of Health Sciences and Technology, Massachusetts Institute of Technology, Cambridge, MA, USA
[b] Department of Electrical Engineering and Computer Science, Massachusetts Institute of Technology, Cambridge, MA, USA

ARTICLE INFO

Article history:
Received 20 June 2011
Available online 2 July 2011

Keywords:
Electroporation
Nanosecond electric pulses
Molecular transport
Drift distance
Propidium
Yo-pro-1

ABSTRACT

Recently there has been intense and growing interest in the non-thermal biological effects of nanosecond electric pulses, particularly apoptosis induction. These effects have been hypothesized to result from the widespread creation of small, lipidic pores in the plasma and organelle membranes of cells (supra-electroporation) and, more specifically, ionic and molecular transport through these pores. Here we show that transport occurs overwhelmingly after pulsing. First, we show that the electrical drift distance for typical charged solutes during nanosecond pulses (up to 100 ns), even those with very large magnitudes (up to 10 MV/m), ranges from only a fraction of the membrane thickness (5 nm) to several membrane thicknesses. This is much smaller than the diameter of a typical cell (~16 μm), which implies that molecular drift transport during nanosecond pulses is necessarily minimal. This implication is not dependent on assumptions about pore density or the molecular flux through pores. Second, we show that molecular transport resulting from post-pulse diffusion through minimum-size pores is orders of magnitude larger than electrical drift-driven transport during nanosecond pulses. While field-assisted charge entry and the magnitude of flux favor transport during nanosecond pulses, these effects are too small to overcome the orders of magnitude more time available for post-pulse transport. Therefore, the basic conclusion that essentially all transmembrane molecular transport occurs post-pulse holds across the plausible range of relevant parameters. Our analysis shows that a primary direct consequence of nanosecond electric pulses is the creation (or maintenance) of large populations of small pores in cell membranes that govern post-pulse transmembrane transport of small ions and molecules.

1. Introduction

In the past decade there has been intense and growing interest in the effects that extremely short duration (<~1 μs), large magnitude (10–100 kV/cm) electric pulses have on cells [1–17]. The effects reported in response to these pulses, such as apoptosis [1–5,8,13,14,16], are generally not seen in response to conventional electroporation pulses and are thought to occur due to electroporation of the plasma membrane and organelle membranes and resultant transport of ions and molecules through these membranes.

To understand and potentially optimize and exploit these nanosecond pulse effects for therapeutic purposes, we must therefore gain a better understanding of the molecular and ionic transport that results from short pulses. To that end, here we address a basic question: When does transmembrane transport predominantly occur for these pulses, during or after pulsing?

We show that the transmembrane transport facilitated by short pulses is dominated by small and weakly charged solutes (due to small pore size and associated hindrance and partitioning) and occurs almost entirely after pulsing. This result, along with experimental observations that large numbers of nanosecond pulses (of order 10–1000) are required to achieve significant effects [5,8,9,13,17], suggests that a primary mechanism by which nanosecond electric pulses affect cells is through the creation (or maintenance) of large populations of small pores that enable post-pulse transmembrane transport of small ions and molecules.

2. Methods

Here we consider approximate descriptions of molecular transport, first based on bulk electrolyte and then on additional estimates that involve pore properties. Our analysis is intentionally simplified, seeking general insight that is essentially independent of cell details.

2.1. Pore creation, expansion, and destruction

Electroporation is a phenomenon in which pores form in lipid bilayers in response to large transmembrane voltage $\Delta\varphi_m$ [18]. Elevated $\Delta\varphi_m$ drives both pore creation and subsequent pore

* Corresponding author. Address: Harvard-M.I.T. Division of Health Sciences and Technology, Massachusetts Institute of Technology, 77 Massachusetts Ave., E25-213A, Cambridge, MA 02139, USA.
E-mail address: jcw@mit.edu (J.C. Weaver).

0006-291X/$ - see front matter © 2011 Elsevier Inc. All rights reserved.
doi:10.1016/j.bbrc.2011.06.171

expansion. However, for nanosecond time scale pulses with magnitudes on the order of several megavolts-per-meter, pore creation predominates in rapidly driving $\Delta\varphi_m$ down to a level ($\sim$0.5 V) at which pore creation and expansion effectively cease [7,15]. As a result, there is very little pore expansion for these pulses [7,12,15], and pores accumulate near pore radius $r_p = r_{p,min} \approx 0.8$ nm [19], the radius at which there is an energy minimum when $\Delta\varphi_m < \sim 0.5$ V [15,20].

Rapid pore creation results in the establishment of a large pore density N in the cell membranes. For short pulses with megavolt-per-meter magnitude, N may reach values up to $\sim 5 \times 10^{16}$ pores/m^2 within a few nanoseconds [6,11]. In our analysis here, the value of N is unimportant and it is sufficient to assume that the initial pore density $N = N_0$ is established immediately and remains constant for the duration of the pulse.

Post-pulse, $N(t)$ is assumed to decay with an exponential resealing time constant (pore lifetime) τ_p:

$$N(t) = N_0 e^{-t/\tau_p}. \quad (1)$$

Reported values for τ_p vary widely, from fractions of a second [21,22] to minutes [23]. Here we use $\tau_p = 1$ s.

2.2. Molecular transport in bulk electrolyte

Molecular transport in bulk electrolyte occurs by unhindered electrodiffusion, the combination of electrical drift and diffusion. The electrodiffusive flux $\boldsymbol{J_s}$ is described by [15,24]

$$\boldsymbol{J_s} = -D_s \nabla\gamma - \frac{D_s}{kT} q_e z_s \gamma \nabla\varphi. \quad (2)$$

Here, γ is solute concentration, φ is electric potential, D_s is solute diffusivity, z_s is solute charge (valence), q_e is elementary charge, k is the Boltzmann constant, and T is absolute temperature. The first term in Eq. (2) describes the flux of solute resulting from a gradient in concentration (diffusion), and the second term describes the flux of solute resulting from a gradient in electric potential (electrical drift).

During the application of a large electric field, molecular transport (for charged solutes) is dominated by electrical drift. The speed v_{drift} at which solute drifts in the presence of an applied electric field with magnitude E is [15,24]

$$v_{drift} = \left(\frac{D_s q_e |z_s|}{kT}\right) E. \quad (3)$$

In time t, the solute drifts distance d_{drift}:

$$d_{drift} = v_{drift} t = \left(\frac{D_s q_e |z_s|}{kT}\right) Et. \quad (4)$$

In the absence of an applied electric field (e.g., following the application of an electric pulse), molecular transport is dominated by diffusion.

2.3. Molecular transport through pores

The electrodiffusive flux equation (Eq. (2)) for bulk electrolyte can be adapted to describe electrodiffusion through pores (Fig. 1) by scaling the flux J_s by the hindrance factor H and the partition factor K [15,25]. That is, the flux $J_{s,p}$ through a pore is related to the flux J_s calculated using bulk electrolyte assumptions (Eq. (2)) by

$$J_{s,p} = HKJ_s. \quad (5)$$

The hindrance factor H ($0 \leqslant H \leqslant 1$) is a function of solute size and pore radius and accounts for the effect that the finite size of a solute has on its interaction with and movement through a pore

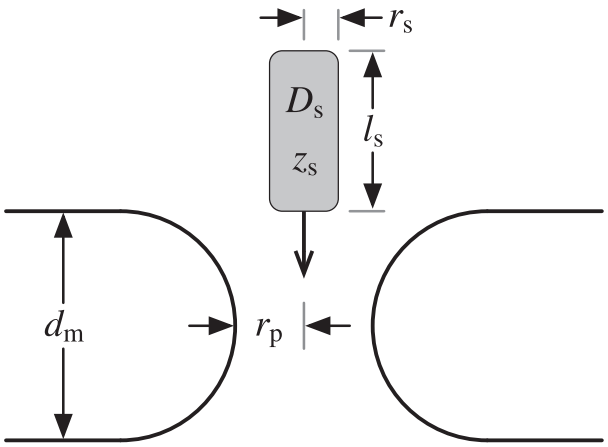

Fig. 1. Movement of a cylindrical molecule through a pore. A cylindrical molecule (solute) with radius r_s and length l_s is shown approaching a pore with radius r_p in a membrane with thickness d_m [15,25]. The transport of a charged molecule in bulk aqueous electrolyte depends on its diffusivity D_s and, in the presence of an electric field, its charge z_s [15,24]. Transport through a pore also depends on the size and shape of the molecule, which determine hindrance, and the charge of the molecule, which determines partitioning [15,25].

[15,25,26]. $H \to 0$ (transport is significantly impeded) when the solute size approaches the pore size, and $H \to 1$ (transport is not significantly impeded) when the solute size is much smaller than the pore size. Here we use the quantitative characterization of hindrance described in Refs. [15,25].

As examples, consider the hindrance factors for yo-pro-1 and propidium for the approximate radius of a minimum-size pore, $r_{p,min} = 0.8$ nm. Yo-pro-1, which can be approximated as a cylinder with radius $r_s = 0.53$ nm and length $l_s = 1.71$ nm [15,27], has $H(r_{p,min}) = 4.0 \times 10^{-3}$. The larger propidium, which can be approximated as a cylinder with radius $r_s = 0.69$ nm and length $l_s = 1.55$ nm [15,27], has smaller $H(r_{p,min}) = 8.3 \times 10^{-5}$. $H(r_{p,min}) \ll 1$ for both solutes, and therefore hindrance greatly diminishes their transport through minimum-size pores.

The partition factor K ($0 \leqslant K \leqslant 1$) is a function of solute charge, pore radius, and transmembrane voltage [15,19,25] and accounts for the effect that the solute charge has on its interaction with and transport through a pore in a low dielectric constant material (e.g., lipid). Here we use the quantitative characterization of partitioning described in Refs. [15,25].

To first order, partitioning only affects charged molecules, and thus $K = 1$ (transport is unimpeded by partitioning) for $z_s = 0$. For $z_s \neq 0$, $K \to 1$ (transport is less impeded) as r_p increases or $\Delta\varphi_m$ increases, and $K \to 0$ (transport is more impeded) as r_p decreases or $\Delta\varphi_m$ decreases. For any given r_p and $\Delta\varphi_m$, K is smaller for solutes with larger $|z_s|$ [15,25].

Again, consider a minimum-size pore ($r_{p,min} = 0.8$ nm). At $\Delta\varphi_m = 0$ V, $K(z_s)$ for several z_s are $K(0) = 1$, $K(\pm1) = 0.51$, $K(\pm2) = 0.053$, $K(\pm3) = 8.9 \times 10^{-4}$, and $K(\pm4) = 2.6 \times 10^{-6}$ [15,25]. At a much larger (supra-physiological) $\Delta\varphi_m = 1$ V, $K(z_s)$ for these same z_s are $K(0) = 1$, $K(\pm1) = 0.91$, $K(\pm2) = 0.83$, $K(\pm3) = 0.74$, and $K(\pm4) = 0.65$ [15,25]. (Note that yo-pro-1 and propidium both have charge $z_s = +2$ [15,27]). Thus, partitioning impedes transport through pores much more significantly when $\Delta\varphi_m = 0$ V (e.g., post-pulse) than when $\Delta\varphi_m = 1$ V (e.g., during pulsing).

In the results and analysis that follow, we characterize transport during a pulse by partition factor K_{during} and characterize transport after a pulse by partition factor K_{after}. K_{during} is calculated for $r_p = r_{p,min} = 0.8$ nm and $\Delta\varphi_m = 1.5$ V, approximately the maximum $\Delta\varphi_m$ reported for experimental [28] and electroporation model [6,7,11,12,14,29] results. K_{after} is calculated for $r_p = r_{p,min} = 0.8$ nm

and $\Delta\varphi_m \approx 0$ V, the transmembrane voltage that persists for many multiples of τ_p following a large electric pulse [11].

3. Results and discussion

3.1. Electrical drift distance during short pulses

The electrical drift distance d_{drift} (Eq. (4)) provides an intuitive means for understanding why molecular uptake during short pulses must be extremely small: If molecules drift only a short distance during a pulse, then it is not possible for many molecules to enter a cell. This is clear in Fig. 2.

Consider a circular plane with area $A_{cell}/2$ (area of one side of a cell with total area A_{cell}) in a standard pulsing medium containing a fluorescent probe (e.g., propidium). An electric field of magnitude E_{pulse} is applied normal to the plane for duration t_{pulse}. The distance d_{drift} through which solute molecules with diffusivity D_s and charge z_s drift during the pulse is (from Eq. (4)).

$$d_{drift} = \left(\frac{D_s q_e |z_s|}{kT}\right) E_{pulse} t_{pulse}. \tag{6}$$

For short pulses, d_{drift} is incredibly small. As an example, consider propidium ($D_s = 42.8 \times 10^{-11}$ m^2/s, $z_s = +2$ [15,27]). For an applied electric pulse with duration $t_{pulse} = 4$ ns and magnitude $E_{pulse} = 8$ MV/m [9] at 25 °C, d_{drift} is only 1.1 nm, a fraction (~0.2) of the membrane thickness ($d_m = 5$ nm). Even for a significantly longer pulse, with duration $t_{pulse} = 60$ ns and magnitude $E_{pulse} = 9.5$ MV/m [28], d_{drift} is just 19 nm, or ~4 times the membrane thickness. Thus, very little solute enters the cell.

The number of molecules that can be delivered to the membrane during a pulse is just $A_{cell} d_{drift} \gamma_e/2$, where γ_e is the extracellular solute concentration (in molecules/m^3). Thus, even if the membrane posed no barrier to transport whatsoever (bulk electrolyte approximation), the relative intracellular concentration γ_i/γ_e immediately following a short pulse would be limited to

$$\frac{\gamma_i}{\gamma_e} \approx \frac{A_{cell} d_{drift}}{2V_{cell}} = \frac{3d_{drift}}{2r_{cell}}. \tag{7}$$

Here, r_{cell} is the radius of a cell with area A_{cell}. Again taking propidium as an example and using a typical $r_{cell} = 8$ μm, in the limit of the membrane posing no barrier to transport, $\gamma_i/\gamma_e \approx 2.0 \times 10^{-4}$ immediately following a 4 ns, 8 MV/m pulse [9] and $\gamma_i/\gamma_e \approx 3.6 \times 10^{-3}$ immediately following a 60 ns, 9.5 MV/m pulse [28]. This is orders of magnitude less transport than can be achieved by conventional electroporation pulses [30].

Moreover, this bound does not consider limited aqueous pore area (<~0.1 [11]), hindrance (~8×10^{-5}), or partitioning (~0.9). Accounting for these factors, the transport would be ~5 orders of magnitude smaller.

Fig. 3 shows the drift distance d_{drift} for a wide range of pulse durations and magnitudes. For illustrative purposes, d_{drift} was calculated using $D_s = 40 \times 10^{-11}$m^2/s (typical of small fluorescent probes [15,27]) and charge $|z_s| = 1$. The results can easily be scaled for other z_s by considering that $d_{drift} \propto z_s$ (Eq. (6)).

3.2. Molecular uptake during short pulses

Here we extend the bulk electrolyte estimates by explicitly considering basic properties of small pores. The number of molecules M_{during} entering a cell during a short pulse can be approximated by

$$M_{during} = \frac{1}{2}(d_{drift}\gamma_e)(A_{cell}A_p N_0)(HK_{during}), \tag{8}$$

where d_{drift} is the drift distance during the pulse (Eq. (6)), γ_e is the extracellular concentration of solute, H is the hindrance factor, K_{during} is the partition factor during the pulse, N_0 is the pore density in the plasma membrane, and A_p ($=\pi r_p^2$) is the aqueous area of a single pore. The first grouped factor, $d_{drift}\gamma_e$, is the number of solute molecules that drift through a region of unit area during the pulse. The second grouped factor, $A_{cell}A_pN_0$, is the total area of pores in the plasma membrane due to pulsing. The third grouped factor, HK_{during}, is the factor by which hindrance and partitioning diminish transport. The 1/2 prefactor accounts for the fact that electrical drift is only directed into the cell for one of its sides.

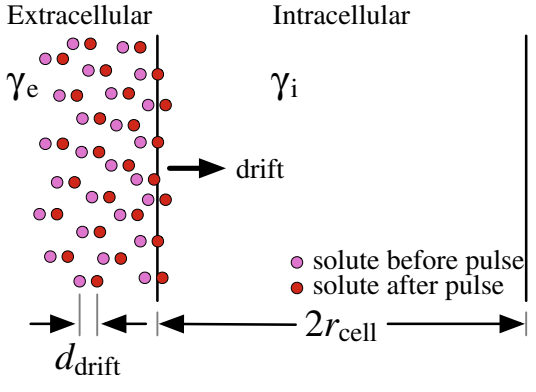

Fig. 2. Electrical drift during short electric pulses. The position of a charged solute is shown before (*pink*) and immediately after (*red*) an electric pulse. During the pulse, the solute drifts a distance d_{drift} (*not to scale*). Because the pulse is short (<~100 ns), d_{drift} is necessarily much smaller than the cell diameter $2r_{cell}$ ($d_{drift} \ll 2r_{cell}$). Consequently, only a small number of solute molecules enter the cell during the pulse, and the increase in the intercellular concentration of solute γ_i during a pulse is much smaller than the extracellular concentration of solute γ_e ($\gamma_i \ll \gamma_e$). (For interpretation of the references to color in this figure legend, the reader is referred to the web version of this article.)

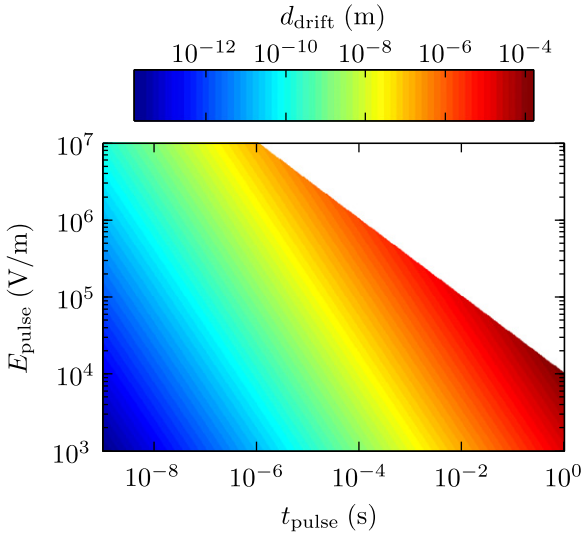

Fig. 3. Electrical drift distance in bulk electrolyte resulting from electric pulses. The electrical drift distance d_{drift} is shown for a range of pulse durations t_{pulse} and magnitudes E_{pulse} for a molecule with diffusivity $D_s = 40 \times 10^{-11}$m^2/s and charge $|z_s| = 1$. d_{drift} is shown only for pulses resulting in a temperature rise $\Delta T \leqslant 25$ °C (assuming 1 S/m electrolyte conductivity and 4.18×10^6 J/(m^3 K) volumetric heat capacity). For pulses resulting in $\Delta T > 25$ °C, d_{drift} is shown as *white*. (Most experimental protocols involve $\Delta T \ll 25$ °C.) For a fixed temperature rise ΔT (e.g., 25 °C), d_{drift} is greater for smaller E_{pulse} because $d_{drift} \propto E_{pulse}$ but $\Delta T \propto E_{pulse}^2$ [15].

3.3. Molecular uptake after short pulses

The number of molecules M_{after} entering a cell after a short pulse (post-pulse) can be approximated by

$$M_{after} = \int_0^{\infty} \left(D_s \frac{\gamma_e - \gamma_i}{d_m} \right) (A_{cell} A_p N(t)) (HK_{after})\, dt, \quad (9)$$

where $N(t) = N_0 \exp(-t/\tau_p)$ (Eq. (1)), γ_i is the intracellular concentration of solute, τ_p is the pore resealing time constant, K_{after} is the partition factor after the pulse, and all other variables are as previously defined. The pore density $N(t)$ is the only time-dependent quantity.

We can assume $\gamma_i \approx 0$ molecules/m^3 because very little molecular transport has been observed following short pulses [9], and even for longer pulses that result in more transport $\gamma_i \ll \gamma_e$ [31].

Taking these considerations into account, Eq. (9) can be simplified to

$$M_{after} = \left(\frac{D_s \tau_p}{d_m} \gamma_e \right) (A_{cell} A_p N_0) (HK_{after}). \quad (10)$$

The form of Eq. (10) is very similar to the form of Eq. (8). The first grouped factor, $D_s \tau_p \gamma_e / d_m$ is the number of solute molecules that diffuse through a region of unit area during one resealing time constant τ_p for a concentration gradient γ_e / d_m. The second grouped factor, $A_{cell} A_p N_0$, is the total area of pores in plasma membrane immediately following the pulse. The third grouped factor, HK_{after}, is the factor by which hindrance and partitioning diminish transport.

3.4. Molecular uptake during versus after short pulses

Assuming drift dominates during a pulse and diffusion dominates after a pulse, the ratio of transport during a pulse to after a pulse can be determined from Eqs. (8) and (10):

$$\frac{M_{during}}{M_{after}} = \frac{1}{2} \left(\frac{d_{drift} d_m}{D_s \tau_p} \right) \left(\frac{K_{during}}{K_{after}} \right). \quad (11)$$

Substituting for d_{drift} (Eq. (6)) and simplifying,

$$\frac{M_{during}}{M_{after}} = \frac{1}{2} \left(\frac{q_e |z_s| E_{pulse} d_m}{kT} \right) \left(\frac{K_{during}}{K_{after}} \right) \left(\frac{t_{pulse}}{\tau_p} \right). \quad (12)$$

Note that M_{during}/M_{after} is independent of H and N_0.

Fig. 4 shows the ratio of molecular uptake during a pulse M_{during} to molecular uptake after a pulse M_{after} for a range of pulse durations and magnitudes. The transport ratio is shown for $|z_s|$ values of 1, 2, 3, and 4 because the partition factors K_{during} and K_{after} are functions of solute charge z_s [15,25]. For all of the conditions considered, $M_{during}/M_{after} \ll 1$. M_{during}/M_{after} is particularly small for the smaller $|z_s|$ values. For any given $|z_s|$, M_{during}/M_{after} is largest for the pulse with $t_{pulse} = 100$ ns and $E_{pulse} = 10$ MV/m. For this pulse, M_{during}/M_{after} is 1.8×10^{-7} for $|z_s| = 1$, 3.2×10^{-6} for $|z_s| = 2$, 2.7×10^{-4} for $|z_s| = 3$, and 0.12 for $|z_s| = 4$.

Consideration of the grouped factors in Eq. (12) provides insight into why M_{during}/M_{after} is so small. The first, $q_e |z_s| E_{pulse} d_m / kT$, is the ratio of drift flux to diffusive flux over a distance d_m. This factor depends on $|z_s|$ and E_{pulse} and is somewhat larger than 1 for typical (relevant) values of these parameters. For example, with $|z_s| = 1$ and $E_{pulse} = 10$ MV/m, the factor is ~19. Thus, this factor favors transport during the pulse.

The second grouped factor in Eq. (12), K_{during}/K_{after}, is the ratio of the partition factor during a pulse to the partition factor after a pulse. This factor depends strongly on $|z_s|$ and is always larger than 1 (field-assisted charge entry) [15,25]. The factor is 1.8 for $|z_s| = 1$, 17 for $|z_s| = 2$, 930 for $|z_s| = 3$, and 3.0×10^5 for $|z_s| = 4$. This factor also favors transport during the pulse, particularly for larger $|z_s|$.

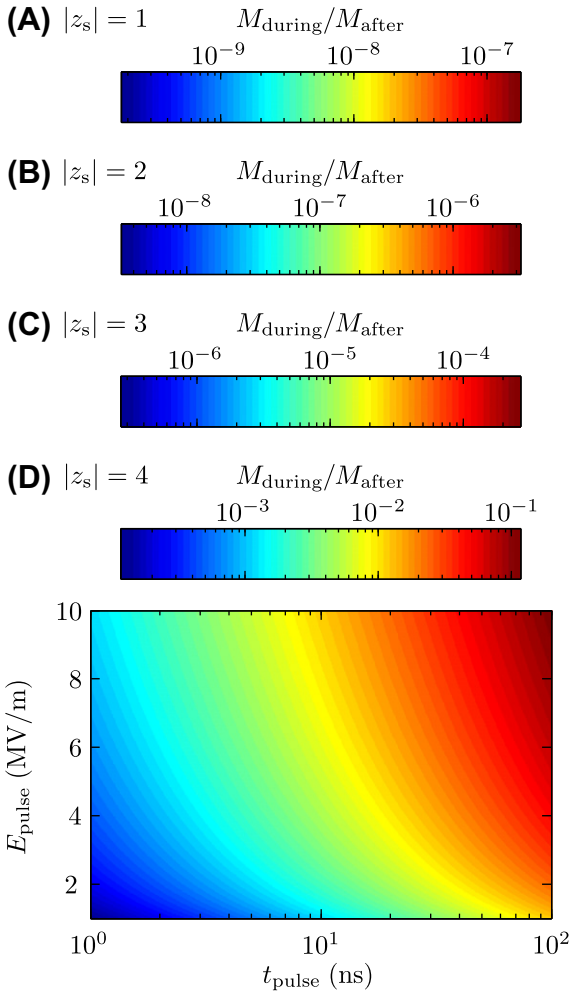

Fig. 4. Molecular uptake during versus after short electric pulses. The ratio of molecular uptake during a pulse M_{during} to molecular uptake after a pulse M_{after} is shown for a range of pulse durations t_{pulse} and magnitudes E_{pulse}. The transport ratio is shown for solute charge values $|z_s|$ of (A) 1, (B) 2, (C) 3, and (D) 4. Note that only the z-axis (colormap) changes with $|z_s|$, and thus the same plot applies for all $|z_s|$. The ratio M_{during}/M_{after} is proportional to t_{pulse} and E_{pulse} and is smaller for smaller values of $|z_s|$. For all of the conditions considered, $M_{during} \ll M_{after}$.

The third grouped factor in Eq. (12), t_{pulse}/τ_p, is the ratio of the pulse duration to the pore resealing time constant. This factor is much smaller than 1. Here we consider pulses with durations $t_{pulse} <\sim 100$ ns, but $\tau_p = 1$ s. Therefore, the ratio $t_{pulse}/\tau_p < 10^{-7}$, and it dominates.

Thus, while the drift flux (during a pulse) exceeds the diffusive flux (after a pulse) over distance d_m and the partition factor during a pulse exceeds, sometimes dramatically, the partition factor after a pulse, these factors simply are too small to compensate for the tiny ratio t_{pulse}/τ_p. In other words, the flux of solute into a cell during a pulse exceeds the flux of solute into a cell after a pulse, but because the duration of a short pulse is so much shorter than the recovery period after a pulse, the vast majority of transport takes place after the pulse.

3.5. Effects of the minimum-size pore radius and resealing time constant values

The value used for the minimum-size pore radius $r_{p,min}$ is important because it affects M_{during}/M_{after} (Eq. (12)) through the partition factors K_{during} and K_{after} [15,25]. Glaser et al. [19] reported that $r_{p,min}$ is in the range 0.6–1.0 nm, and the average of $r_{p,min} = 0.8$ nm has been widely used in mathematical models of

electroporation (e.g., Refs. [12,32]). According to Barnett et al. [20], packing constraints require that $r_{p,min} > \sim 0.7$ nm, and they used $r_{p,min} = 1.0$ nm in their model. In a recent study [15,25] in which we analyzed the bilayer lipid membrane conductance measurements by Melikov et al. [21], we found $r_{p,min} \approx 1.0$ nm. Nonetheless, in the interest of taking a conservative approach, here we employed the widely used $r_{p,min} = 0.8$ nm.

The extent to which changing $r_{p,min}$ affects K_{during}/K_{after} (and therefore M_{during}/M_{after}) depends on the solute charge z_s. For $|z_s| = 4$, decreasing $r_{p,min}$ to 0.7 nm increases K_{during}/K_{after} by a factor of 36, and increasing $r_{p,min}$ to 0.9 nm decreases K_{during}/K_{after} by a factor of 12. The effect of changing $r_{p,min}$ on K_{during}/K_{after} for smaller $|z_s|$ is much less significant. Thus, using other larger or smaller values of $r_{p,min}$ would not affect our general conclusion that $M_{during} \ll M_{after}$.

The value used for the pore resealing time constant τ_p is also important because it directly affects M_{during}/M_{after} (Eq. (12)). Literature values of τ_p vary widely. While Glaser et al. [19] reported $\tau_p \approx 3$ s and He et al. [33] reported $\tau_p \approx 0.8–2.2$ s, Tekle et al. [22] reported a shorter $\tau_p \approx 0.16$ s and Djuzenova et al. [23] reported a much longer $\tau_p \approx 60–120$ s. Here we used $\tau_p \approx 1$ s, which is on the lower end of the range of experimentally determined values for cells. Decreasing τ_p would decrease M_{during}/M_{after}, and increasing τ_p would increase M_{during}/M_{after}. While reported values of τ_p vary widely, they do not vary widely enough to change our general conclusion that $M_{during} \ll M_{after}$.

4. Conclusions

This analysis strongly suggests that the vast majority of molecular transport that results from nanosecond electric pulses ($<\sim$100 ns) occurs post-pulse. Indeed, the transport during these pulses appears to be negligible. While simplifying assumptions were made in this analysis and some uncertainty exists in a few of the parameters, the overall estimates appear conservative.

We therefore conclude that a primary consequence of extremely large, nanosecond electric pulses is the creation (or maintenance) of large populations of small membrane pores that facilitate post-pulse transmembrane transport of small ions and molecules.

Acknowledgments

We thank T.R. Gowrishankar and R.S. Son for valuable discussions and K.G. Weaver for computer assistance.

This work was supported by the National Institutes of Health (Grant No. GM063857) and graduate research fellowships from the National Science Foundation and the Harvard-M.I.T. Division of Health Sciences and Technology.

References

[1] K.H. Schoenbach, S.J. Beebe, E.S. Buescher, Intracellular effect of ultrashort electrical pulses, Bioelectromagnetics 22 (2001) 440–448.
[2] S.J. Beebe, J. White, P.F. Blackmore, Y.P. Deng, K. Somers, K.H. Schoenbach, Diverse effects of nanosecond pulsed electric fields on cells and tissues, DNA Cell Biol. 22 (2003) 785–796.
[3] P.T. Vernier, Y.H. Sun, L. Marcu, S. Salemi, C.M. Craft, M.A. Gundersen, Calcium bursts induced by nanosecond electric pulses, Biochem. Biophys. Res. Commun. 310 (2003) 286–295.
[4] K.H. Schoenbach, R.P. Joshi, J.F. Kolb, N.Y. Chen, M. Stacey, P.F. Blackmore, et al., Ultrashort electrical pulses open a new gateway into biological cells, P IEEE 92 (2004) 1122–1137.
[5] A.G. Pakhomov, A. Phinney, J. Ashmore, K. Walker, J.F. Kolb, S. Kono, et al., Characterization of the cytotoxic effect of high-intensity, 10-ns duration electrical pulses, IEEE T Plasma Sci. 32 (2004) 1579–1586.
[6] T.R. Gowrishankar, A.T. Esser, Z. Vasilkoski, K.C. Smith, J.C. Weaver, Microdosimetry for conventional and supra-electroporation in cells with organelles, Biochem. Biophys. Res. Commun. 341 (2006) 1266–1276.
[7] Z. Vasilkoski, A.T. Esser, T.R. Gowrishankar, J.C. Weaver, Membrane electroporation: the absolute rate equation and nanosecond time scale pore creation, Phys. Rev. E. 74 (2006) 021904.
[8] R. Nuccitelli, U. Pliquett, X.H. Chen, W. Ford, R.J. Swanson, S.J. Beebe, et al., Nanosecond pulsed electric fields cause melanomas to self-destruct, Biochem. Biophys. Res. Commun. 343 (2006) 351–360.
[9] P.T. Vernier, Y.H. Sun, M.A. Gundersen, Nanoelectropulse-driven membrane perturbation, small molecule permeabilization, BMC Cell Biol 7 (2006) 37.
[10] Y. Sun, P. Vernier, M. Behrend, J. Wang, M. Thu, M. Gundersen, et al., Fluorescence microscopy imaging of electroperturbation in mammalian cells, J. Biomed. Opt. 11 (2006) 024010.
[11] K.C. Smith, J.C. Weaver, Active mechanisms are needed to describe cell responses to submicrosecond, megavolt-per-meter pulses: Cell models for ultrashort pulses, Biophys. J. 95 (2008) 1547–1563.
[12] A.T. Esser, K.C. Smith, T.R. Gowrishankar, J.C. Weaver, Towards solid tumor treatment by nanosecond pulsed electric fields, Technol Cancer Res T. 8 (2009) 289–306.
[13] R. Nuccitelli, K. Tran, S. Sheikh, B. Athos, M. Kreis, P. Nuccitelli, Optimized nanosecond pulsed electric field therapy can cause murine malignant melanomas to self-destruct with a single treatment, Int. J. Cancer 127 (2010) 1727–1736.
[14] R.P. Joshi, K.H. Schoenbach, Bioelectric effects of intense ultrashort pulses, Crit. Rev. Biomed. Eng. 38 (2010) 255–304.
[15] K.C. Smith, A Unified Model of Electroporation and Molecular Transport, Massachusetts Institute of Technology, Cambridge, Massachusetts, 2011.
[16] W. Ren, S.J. Beebe, An apoptosis targeted stimulus with nanosecond pulsed electric fields (nsPEFs) in E4 squamous cell carcinoma, Apoptosis 16 (2011) 382–393.
[17] B.L. Ibey, C.C. Roth, A.G. Pakhomov, J.A. Bernhard, G.J. Wilmink, O.N. Pakhomova, Dose-Dependent Thresholds of 10-ns Electric Pulse Induced Plasma Membrane Disruption and Cytotoxicity in Multiple Cell Lines, PLoS One 6 (2011) e15642.
[18] J.C. Weaver, Y.A. Chizmadzhev, Theory of electroporation: a review, Bioelectroch. Bioener. 41 (1996) 135–160.
[19] R.W. Glaser, S.L. Leikin, L.V. Chernomordik, V.F. Pastushenko, A.I. Sokirko, Reversible electrical breakdown of lipid bilayers: Formation and evolution of pores, Biochim. Biophys. Acta. 940 (1988) 275–287.
[20] A. Barnett, J.C. Weaver, Electroporation–A unified, quantitative theory of reversible electrical breakdown and mechanical rupture in artificial planar bilayer-membranes, Bioelectroch. Bioener. 25 (1991) 163–182.
[21] K.C. Melikov, V.A. Frolov, A. Shcherbakov, A.V. Samsonov, Y.A. Chizmadzhev, L.V. Chernomordik, Voltage-induced nonconductive pre-pores and metastable single pores in unmodified planar lipid bilayer, Biophys. J. 80 (2001) 1829–1836.
[22] E. Tekle, R.D. Astumian, W.A. Friauf, P.B. Chock, Asymmetric pore distribution and loss of membrane lipid in electroporated DOPC vesicles, Biophys. J. 81 (2001) 960–968.
[23] C.S. Djuzenova, U. Zimmermann, H. Frank, V.L. Sukhorukov, E. Richter, G. Fuhr, Effect of medium conductivity and composition on the uptake of propidium iodide into electropermeabilized myeloma cells, Biochim. Biophys. Acta 1284 (1996) 143–152.
[24] K.C. Smith, J.C. Weaver, Electrodiffusion of molecules in aqueous media: A robust, discretized description for electroporation and other transport phenomena (accepted), IEEE T Bio-Med. Eng.
[25] K.C. Smith, J.C. Weaver, Effects of hindrance and partitioning on ionic and molecular transport through small lipidic pores (submitted).
[26] P.M. Bungay, H. Brenner, The motion of a closely-fitting sphere in a fluid-filled tube, Int. J. Multiphas Flow 1 (1973) 25–56.
[27] K.C. Smith, J.C. Weaver, Computation and compilation of the size, charge, and diffusivity of fluorescent dyes and other molecules (submitted).
[28] W. Frey, J.A. White, R.O. Price, P.F. Blackmore, R.P. Joshi, R. Nuccitelli, et al., Plasma membrane voltage changes during nanosecond pulsed electric field exposure, Biophys. J. 90 (2006) 3608–3615.
[29] K.C. Smith, T.R. Gowrishankar, A.T. Esser, D.A. Stewart, J.C. Weaver, The spatially distributed dynamic transmembrane voltage of cells and organelles due to 10-ns pulses: Meshed transport networks, IEEE T Plasma Sci. 34 (2006) 1394–1404.
[30] P.J. Canatella, J.F. Karr, J.A. Petros, M.R. Prausnitz, Quantitative study of electroporation-mediated molecular uptake and cell viability, Biophys. J. 80 (2001) 755–764.
[31] M.R. Prausnitz, B.S. Lau, C.D. Milano, S. Conner, R. Langer, J.C. Weaver, A quantitative study of electroporation showing a plateau in net molecular-transport, Biophys. J. 65 (1993) 414–422.
[32] W. Krassowska, P.D. Filev, Modeling electroporation in a single cell, Biophys. J. 92 (2007) 404–417.
[33] H. He, D.C. Chang, Y. Lee, Nonlinear current response of micro electroporation and resealing dynamics for human cancer cells, Bioelectrochemistry 72 (2008) 161–168.